STM JOURNALS

Journal of
Polymer & Composites

ISSN: 2321-2810 (Online)
ISSN: 2321-8525 (Print)
Volume 13, Special Issue 6, 2025
DOI (Journal): 10.37591/JoPC

https://journals.stmjournals.com/jopc

Research JoPC

Experimental Analysis of Aramid Fiber Reinforced with Tungsten Carbide

Prashant Manvi[1,*], Siddalingappa P. Kodigaddi[2], Srikanth H.V.[3], Rachitha A[4], Aswin Sidharth M.[5], Ullas Gowda A.[6]

Abstract

This study investigates the mechanical performance of aramid fiber-reinforced epoxy composites enhanced with varying weight percentages of tungsten carbide (WC) powder as a secondary reinforcement. The composites were fabricated using both the hand lay-up and vacuum bagging techniques to ensure uniform dispersion of materials and quality surface finish. Tungsten carbide particles with an average size of 4 microns were incorporated into the aramid fiber matrix at incremental concentrations of 0%, 5%, 10%, 15%, and 20% by weight. The aim was to evaluate the influence of WC loading on key mechanical properties such as tensile strength, yield load, elongation at yield, and elongation at break. Experimental results revealed a progressive enhancement in tensile properties with increasing WC content. Among all the compositions, the composite containing 20% tungsten carbide demonstrated the highest mechanical performance, exhibiting a peak tensile strength of 359.68 N/mm² and a peak load of 22.48 kN, surpassing all other formulations. This optimized performance can be attributed to the effective load distribution and interfacial bonding between the aramid fibers and the hard WC particles. The composite with 15% WC displayed slightly lower tensile strength but recorded the highest elongation at break, suggesting a favorable trade-off between stiffness and ductility. The findings confirm that tungsten carbide significantly enhances the structural integrity of aramid fiber composites, with 20% WC emerging as the most effective filler ratio. These results indicate the potential of such hybrid composites for applications requiring high strength, wear resistance, and thermal stability, such as in defense and structural engineering.

Keywords: Aramid Fiber, Tungsten Carbide, Epoxy, Vacuum bagging, composite

INTRODUCTION

Composite materials, composed of two or more distinct phases—typically a fiber and a matrix—are engineered to provide superior performance by combining the desirable properties of the individual constituents. Composites provide several advantages over conventional materials, including superior strength-to-weight ratios, resistance to corrosion, and greater design flexibility. These properties make them highly suitable for use in aerospace, automotive, civil infrastructure, and defense industries. [1], [2]. Among high-performanc e fibers, aramid fibers (aromatic polyamides) are widely used due to their exceptional tensile strength, impact resistance, and thermal stability. Kevlar and Nomex, two well-known aramid variants, are commonly employed in ballistic armor, aircraft panels, and high-performance sports equipment [3–5]. Their high melting points (>500°C) and strong inter-chain

***Author for Correspondence**
Prashant Manvi

[1,2]Assistant Professor, Department of Aeronautical Engineering, Nitte Meenakshi Institute of Technology (NMIT), Bengaluru, Karnataka, India
[3]Professor, Department of Aeronautical Engineering, Nitte Meenakshi Institute of Technology (NMIT), Bengaluru, Karnataka, India
[4-6]Students, Department of Aeronautical Engineering, Nitte Meenakshi Institute of Technology (NMIT), Bengaluru, Karnataka, India

Received Date: March 26, 2024
Accepted Date: June 10, 2025
Published Date: September 04, 2025

Citation: Prashant Manvi, Siddalingappa P. Kodigaddi, Srikanth H V., Rachitha A, Aswin Sidharth M., Ullas Gowda A. Experimental Analysis of Aramid Fiber Reinforced with Tungsten Carbide. Journal of Polymer & Composites. 2025; 13(Special Issue 6): S146–S157p.

hydrogen bonding make them resilient in extreme environments. The orientation of molecular chains along the fiber axis results in exceptional load-bearing capacity [6]. Epoxy resins are the matrix of choice in many structural composites due to their excellent adhesion, low shrinkage, dimensional stability, and compatibility with fibers. The use of appropriate curing agents and additives further enhances their mechanical, thermal, and chemical performance [7, 8]. In recent years, there has been growing interest in hybrid composites, which incorporate both fibers and fillers to fine-tune mechanical and tribological properties. The addition of micro- and nano-fillers to fiber-reinforced polymer (FRP) composites can significantly enhance wear resistance, stiffness, thermal stability, and fracture toughness [9, 10]. Notably, ceramic and metallic fillers like SiC, Al_2O_3, graphene, and tungsten carbide have been investigated for such enhancements [11–14]. Tungsten carbide (WC), a ceramic known for its exceptional hardness, wear resistance, and thermal conductivity, is a promising reinforcement for polymer composites in applications demanding abrasion resistance and mechanical durability [15]. However, limited studies have focused on its integration into aramid fiber-reinforced epoxy systems, particularly with varying filler weight percentages. The current study aims to investigate the mechanical performance of aramid fiber-reinforced epoxy composites enhanced with tungsten carbide powder. Composites were fabricated using both hand layup and vacuum bagging techniques, and mechanical tests were performed on specimens with WC concentrations of 0%, 5%, 10%, 15%, and 20%. Similar studies involving hybrid reinforcement techniques using SiC, TiO_2, CNTs, and graphene nanoplatelets (GNPs) have demonstrated notable improvements in stiffness, impact resistance, and load-bearing capacity [16–20]. This research seeks to bridge the knowledge gap by offering experimental evidence on the effectiveness of tungsten carbide-filled aramid composites, with a focus on tensile strength and structural integrity optimization for potential engineering applications.

METHODOLOGY

Selection of Materials

Aramid fibers were high-performance synthetic fibers known for their exceptional tensile strength and modulus, which made them ideal for reinforcing composites. On a weight-for-weight basis, aramid fibers exhibited significantly superior mechanical properties compared to steel and fiberglass, including higher strength and lower density. Their outstanding heat and flame resistance, along with their mechanical robustness, led to widespread use in the aerospace and defense industries, such as in aircraft components and protective gear. The molecular structure of aramid fibers featured long-chain polyamides with aromatic rings and amide groups, resulting in a rigid, rod-like backbone. These chains were interconnected by strong hydrogen bonds, which efficiently transmitted mechanical stress and allowed for the use of relatively low molecular weight chains. The alignment of chemical bonds along the fiber axis further enhanced their strength and flexibility. Aramid fibers demonstrated excellent thermal stability, retaining much of their strength at elevated temperatures and decomposing only around 500°C (carbonizing at approximately 425°C). Additional advantages included low flammability, resistance to organic solvents, and good fatigue and chemical resistance, although they were sensitive to strong acids and UV exposure. These properties collectively made aramid fibers indispensable in demanding applications where strength, durability, and heat resistance were critical.

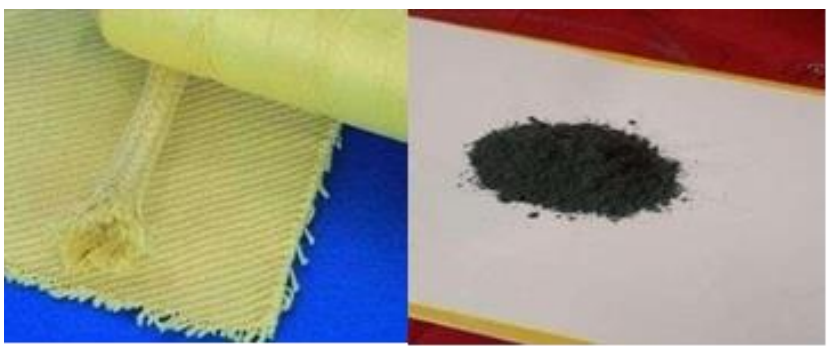

Figure 1. Aramid Fiber and Tungsten carbide.

Aramid fibers were utilized to reinforce composites due to their high tensile modulus and strength. When compared by weight, they exhibited significantly superior mechanical properties than steel and fiberglass. Additionally, aramid fibers possessed excellent heat and fire resistance, which expanded their use in the aerospace and defense industries. Their molecular structure featured hydrogen bonds that efficiently transferred mechanical stress, enabling the use of relatively low molecular weight chains. The chemical bonds were aligned along the fiber axis, providing enhanced strength and flexibility. These fibers also demonstrated outstanding heat resistance, low flammability, and strong resistance to organic solvents, with decomposition beginning at around 500 °C [4]. Tungsten carbide was roughly twice as dense as steel. It was produced by heating a mixture of tungsten and carbon at high temperatures—often using plasma—followed by cooling in an inert gas atmosphere. This process yielded a fine microstructure that imparted exceptional hardness and durability compared to other tungsten carbide compounds. However, due to its metastable nature, the compound's stability decreased at elevated temperatures. Tungsten carbide had a high melting point of about 3,140 K and a boiling point of approximately 6,270 K. It was extremely hard, with a Mohs hardness of 9–9.5, an ultimate tensile strength of 344 MPa, and a Poisson's ratio of 0.31. Aramid Fiber and Tungsten carbide used in this study are as shown in Figure 1.

Fabrication of Materials

The fabrication of aramid fiber was carried out through the following steps:

- *Fiber Preparation:* The aramid fiber was measured and cut according to the required dimensions. Abro tape was applied to the edges of the fiber to prevent damage. The cut fiber was then used for fabrication, and its weight was recorded.
- *Matrix Preparation:* The matrix used was a combination of epoxy resin and hardener. The quantity of the matrix was calculated based on the weight of the cut fiber. Resin was taken at 100% of the fiber's weight, and hardener was added at 10% of the fiber's weight. The resin and hardener were mixed thoroughly using a mechanical stirrer.
- *Resin Application:* The prepared resin-hardener mixture was uniformly applied to the fiber, ensuring that all parts of the fiber were properly wet.
- *Peel Ply and Breather Application:* After resin application, the aramid fiber was wrapped with a peel ply, which facilitated easy separation from the breather after the curing phase. A breather layer was then applied over the peel ply to absorb excess resin and to ensure a well-laminated fabrication.
- *Curing:* The wrapped fiber was placed inside a sealed vacuum bag connected to a vacuum pump. The pump was used to evacuate air from the bag to achieve the desired pressure. The vacuum bag was inspected for leaks, and the curing process was allowed to continue for approximately 5 to 6 hours.

Vacuum Bagging

Vacuum bagging is a process that uses atmospheric pressure to hold together adhesive- or resin-coated components during lamination, ensuring they remain securely in place until the adhesive cures completely. This efficient technique enables the lamination of a wide variety of materials, including traditional wood veneers as well as modern synthetic fibers and core materials.

Vacuum Bagging Materials

Release Fabric

The wet laminate must be directly covered with the release fabric. The necessity for surface pretreatment prior to secondary bonding is decreased by the removable fabric's ability to leave behind a textured surface following removal.[22] Peel ply is the common name for the fabric that peels off fibers and vacuum bags. Nylon or polyester fibers are used to make the most popular kinds of shell layers. Release agents have been applied to some shell layers.

Release Film

A thin plastic material called perforated release film has tiny pores that help stop excess epoxy from transferring from the part to the breather fabric. This vacuum bagging step has an optional layer.

Breather Material

The permeable fabric actually serves two purposes. The extruded epoxy penetrates the skin layer (and any release film you're using, if any) and into the breather fabric as the vacuum pressure strengthens the laminate. Air can easily pass through the breather fabric's open structure, which permits air to escape from the closed lamination.

Sealant Tape

A space should be left between the sealing tape and the laminate when you wrap it around the piece's edge. The area where the tape will be applied needs to be neat and free of fibers and epoxy residue. Adhesive tape and sealing compound are other names for sealing tape.

Vacuum Bag

A vacuum bag (Figure 2) is made of plastic film that has been sealed inside of a mold. Due to the part's curvature, this layer must be cut too large. Most of the time, the vacuum bag makes up half of the airtight enclosure around the laminate. 6-mil polyethylene plastic can be utilized for the bag if vacuum pressure less than 5 psi (10 hg) will be employed at room temperature. To make it simple to inspect the laminates while it dries. Vacuum bag material that has been carefully made should be utilized for applications that require higher pressure and temperature.

The Plumbing System: The vacuum pump (Figure 3) may extract air and lower the air pressure in the vacuum shell because the piping system creates an air tight passage from the vacuum shell to the vacuum pump. A rigid pipe or flexible hose, a lock, and a gate that joins the pipe to the body make up the fundamental components of the system. In a more adaptable system, the vacuum pressure of the envelope inside the casing is controlled by a control valve and a vacuum control valve. The system may have some kind of ductwork to help route air to a single port, or it may be split to generate numerous ports for big laminates. Table 1 contains the materials data used in this research.

Specimen Preparation

The aramid fiber was cut into dimensions of 300 mm × 300 mm. Abro tape was applied to the edges of the fiber to prevent fraying. The matrix was then prepared by initially mixing epoxy resin and hardener in a 10:1 ratio. Tungsten carbide (WC) powder was added to this mixture in the required amount, and the mixture was stirred thoroughly until it became homogeneous. A total of five layers of aramid fiber were fabricated. Each layer was weighed before use. The homogeneous resin-hardener-WC mixture was uniformly applied to each layer of fiber, ensuring complete wetting. The same procedure was repeated for all subsequent layers.

Figure 2. Vacuum Bag.

Figure 3. Vacuum pump.

Table 1. Materials Data.

Fiber used	Aramid Fiber
Resin used	ARALDITE LY556 IN
Hardener used	ARADUR HY951
Powder	4-micron Tungsten carbide powder
Fiber Dimension	300mmx300mm
Epoxy and Hardener ratio	10:1
Fiber Layers	5 Layers
Vacuum time	6 hours

For the second specimen, tungsten carbide powder equal to 5% of the total fiber weight was added to the resin-hardener mixture and stirred until it reached a homogeneous consistency. The mixture was then applied uniformly to the fiber, as shown in Figure 4. The same process was followed for the remaining specimens, with 10%, 15%, and 20% of WC powder (relative to the total fiber weight) being added to the mixture and applied to the respective fiber layers. After resin application, the laminated fibers were placed in a vacuum bag and subjected to pressure using a vacuum pump to ensure proper compaction and lamination. The curing time for the aramid fiber laminates was approximately 6 hours.

Kevlar para-aramid is an aromatic polyamide distinguished by its long, rigid, and crystalline polymer chains. It can be used alone or combined with composite materials to enhance strength. Kevlar is widely employed in bulletproof vests and body armor, as well as in reinforcement applications for car tires, brakes, and the structural components of cars, boats, and aircraft. In this study, a medium-viscosity, unmodified epoxy resin based on bisphenol-A, known as Araldite LY 566 from Huntsman, was used as the matrix material. The Kevlar fabric layers were bonded using Araldite, a registered trademark of Huntsman LLC. To cure the epoxy resin, a curing agent—also known as a hardener—was added. The hardener used in this study was a low-viscosity cycloaliphatic polyamine, known as Hardener HY 951. A higher resin-to-hardener ratio is typically adopted when a curing agent is incorporated. In this study, a resin-to-hardener ratio of 10:1 was employed. HY 951 was selected to enhance the strength and adhesive properties of the composite. It is a colorless liquid hardener with a characteristic ammonia-like odor due to its pH. One of the most thermodynamically stable forms of tungsten carbide is macrocrystalline, which is widely used in products such as hardfacing rods, wear components, saw blades, mining and construction tools, thermal spray powders, and diamond infiltration tools [21]. The tungsten carbide powder used in this experiment had a crystal size of 3–4 microns. In the fabrication process, epoxy resin, hardener, and tungsten carbide powder were combined to produce the aramid fiber composite laminates. A total of 90 grams of aramid fiber was used. The details of the weight of the fiber and other mixture compositions used are as given in Table 2.

Figure 4. Fabrication of laminates.

Table 2. The following table contains the weight of the fiber and other mixture compositions used in the experiment.

Sl. No	Aramid fiber weight (g)	Epoxy and hardener ratio	Weight of TC powder %
1	90	10:1	0
2	90	10:1	5
3	90	10:1	10
4	90	10:1	15
5	90	10:1	20

After measuring the materials to the required accuracy, the epoxy resin and hardener were thoroughly mixed for approximately 4 to 5 minutes. Initially, the fabrication was carried out without using tungsten carbide powder (0%). The mixture was properly spread over the fiber, and layers of cut fiber were applied. Experiments were conducted using 0%, 5%, 15%, and 20% tungsten carbide powder mixed with the resin and hardener. WC is added to aramid fiber composites in incremental steps (0%, 5%, 10%) to systematically evaluate mechanical improvements. Studies show that 5–10 wt% WC significantly enhances tensile strength, hardness, and wear resistance [23]. However, higher loadings (>10–20 wt%) can cause brittleness, porosity, and particle clustering, reducing overall toughness [24]. The 5–10 wt% range is often optimal, offering improved strength without compromising processability [25]. Lower percentages (1–4 wt%) in other systems, like concrete, also show linear gains in strength [26]. Stepwise additions enable statistical clarity (e.g., ANOVA), supporting effective optimization of composite performance [27]. Cut specimens for the 0%, 5% 15% and 20% Tungsten carbide are as shown in Figure 5 and 6.

TESTING AND RESULTS

Tensile testing was performed using a 100 kN Computerized Universal Testing Machine (UTM). In accordance with the ASTM standard for tensile specimens, the samples were cut to dimensions of 25 mm in length and 2.5 mm in width. The test specimens were positioned between the UTM grips and loaded until the crosshead travel (CHT) limit was reached. Five samples of each configuration were used, and the process was repeated to ensure consistency. Table 3 presents the total number of layers fabricated, the percentage of tungsten carbide used, and the total number of specimens tested.

Figure 5. Cut specimens (0%, 5% Tungsten carbide).

Figure 6. Cut specimens (15%, 20% Tungsten carbide).

Table 3. Specimens Used for Testing.

Model No.	Description
5L-0%TC-01	5 Layer without Tungsten Carbide Powder
5L-0%TC-02	
5L-0%TC-03	
5L-0%TC-04	
5L-0%TC-05	
5L-5%TC-01	5 Layer with 5% of Tungsten Carbide Powder
5L-5%TC-02	
5L-5%TC-03	
5L-5%TC-04	
5L-5%TC-05	
5L-10%TC-01	5 Layer with 10% of Tungsten Carbide Powder
5L-10%TC-02	
5L-10%TC-03	
5L-10%TC-04	
5L-10%TC-05	
5L-15%TC-01	5 Layer with 15% of Tungsten Carbide Powder
5L-15%TC-02	
5L-15%TC-03	
5L-15%TC-04	
5L-15%TC-05	
5L-20%TC-01	5 Layer with 20% of Tungsten Carbide Powder
5L-20%TC-02	
5L-20%TC-03	
5L-20%TC-04	
5L-20%TC-05	

The cut specimens of aramid fiber laminates were tested using a Universal Testing Machine, as shown in Figures 7 and 8. The Load at Yield (LY), Elongation at Yield (EY), Load at Peak (LP), Tensile Strength (TS), and Elongation at Break (EB) were determined for aramid fiber specimens containing 0%, 5%, 10%, 15%, and 20% tungsten carbide powder. The results were tabulated accordingly. The table below presents the data obtained from testing the aramid fiber specimen with 0% tungsten carbide powder under the UTM, with all measurements conducted in accordance with ASTM standards.

Table 4. 0% Tungsten Carbide Results

SL No	Load at yield (kN)	Elongation at yield (mm)	Load at peak (kN)	Tensile Strength (N/mm^2)	Elongation at break (mm)
01	15.95	8.22	19.95	319.20	11.24
02	15.75	7.17	19.75	316.00	9.73
03	14.30	7.06	17.90	286.40	10.58
04	14.65	7.64	18.35	293.60	11.40
05	14.00	7.81	18.22	289.60	11.91
Average	**14.93**	**7.58**	**18.83**	**300.96**	**10.97**

Figure 7. Tested specimens (0% and 5% tungsten carbide).

Figure 8. Tested specimens (15% and 20% tungsten carbide).

Table 5. 5% Tungsten Carbide Results

SL No	Load at yield (kN)	Elongation at yield (mm)	Load at peak (kN)	Tensile Strength (N/mm²)	Elongation at break (mm)
01	15.15	7.34	8.95	303.20	8.77
02	16.05	7.80	20.10	312.60	11.65
03	15.35	7.29	18.05	313.80	11.45
04	15.15	8.13	19.70	298.20	11.90
05	15.40	7.51	18.75	301.20	11.69
Average	**15.42**	**7.61**	**19.11**	**307.60**	**11.09**

Table 6. 10% Tungsten Carbide Results.

SL No	Load at yield (kN)	Elongation at yield (mm)	Load at peak (kN)	Tensile Strength (N/mm²)	Elongation at break (mm)
01	18.75	8.33	23.45	375.20	10.25
02	17.20	7.29	21.55	344.80	11.48
03	16.40	8.75	20.55	328.80	11.36
04	15.25	7.22	19.10	305.60	12.39
05	16.20	7.39	20.30	324.80	11.78
Average	**16.76**	**7.796**	**20.99**	**335.84**	**11.45**

Table 7.15% Tungsten Carbide Results

SL No	Load at yield (kN)	Elongation at yield (mm)	Load at peak (kN)	Tensile Strength (N/mm²)	Elongation at break (mm)
01	16.55	7.90	20.70	331.20	11.04
02	20.20	8.36	25.25	404.00	12.19
03	15.15	7.39	18.95	303.20	10.9
04	16.10	8.46	18.95	303.20	11.88
05	13.60	6.56	17.05	272.80	11.04
Average	**16.32**	**7.734**	**20.18**	**322.88**	**11.42**

Table 8. 20% Tungsten Carbide Results.

SL No	Load at yield (kN)	Elongation at yield (mm)	Load at peak (kN)	Tensile Strength (N/mm²)	Elongation at break (mm)
01	17.80	8.110	22.30	356.80	11.19
02	17.70	8.150	22.20	355.20	11.65
03	15.85	7.240	19.85	317.60	11.44
04	18.30	8.160	22.90	366.40	11.51
05	20.10	7.850	25.15	402.40	11.69
Average	**17.95**	**7.902**	**22.48**	**359.68**	**11.49**

Table 9. Summary of Mechanical Properties vs. WC Content.

WC (%)	Load at Yield (kN)	Elongation at Yield (mm)	Load at Peak (kN)	Tensile Strength (N/mm²)	Elongation at Break (mm)
0	14.93	7.58	18.83	300.96	10.97
5	15.42	7.61	19.11	307.60	11.09
10	16.76	7.80	20.99	335.84	11.45
15	16.32	7.73	20.18	322.88	11.42
20	17.95	7.90	22.48	359.68	11.50

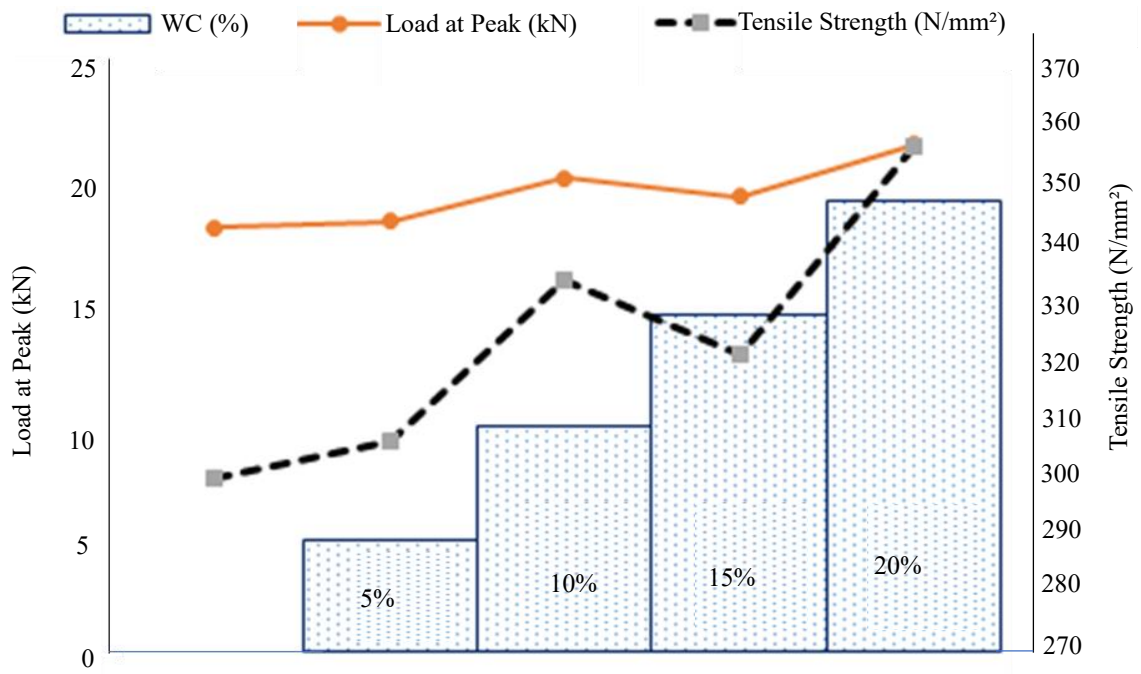

Figure 9. Comparison of mechanical properties for various WC.

Tables 4 to 9 show the results for 0% to 20% Tungsten Carbide Aramid fiber under UTM, in which measurements were followed according to ASTM standard. The tensile performance of aramid fiber composites improved with the addition of WC up to 20%. At 0% WC, the baseline tensile strength averaged 300.96 N/mm², with moderate elongation at break (10.97 mm). With 5% WC, there was a slight increase in strength (307.60 N/mm²) and elongation, indicating improved load distribution and fiber–matrix bonding. A notable enhancement occurred at 10% WC, where the tensile strength peaked at 335.84 N/mm² and elongation at break reached 11.45 mm, reflecting optimal reinforcement without embrittlement. This trend began to reverse at 15% WC, where the average tensile strength dropped to 322.88 N/mm², despite some high individual values, suggesting inconsistency possibly due to particle agglomeration. At 20% WC, strength increased again to 359.68 N/mm², the highest among all samples, while maintaining good ductility (11.50 mm average elongation). This suggests that with proper dispersion, higher WC loading can enhance both strength and toughness. However, process control becomes critical at this level to avoid clustering. Overall, 10–20% WC shows the most effective improvement in mechanical properties, with 10% offering optimal consistency and balance, and 20% demonstrating peak performance with some risk of variability. The tensile test results of aramid fiber composites reinforced with varying WC content (0–20%) show a clear trend in mechanical performance improvement. As WC content increases, both load at yield and load at peak rise, indicating enhanced strength. Notably, tensile strength improves steadily from 300.96 N/mm² (0%) to 359.68 N/mm² (20%), showing the reinforcing effect of WC particles. Elongation at break also slightly increases, peaking at 11.50 mm at 20% WC, suggesting that ductility is maintained or marginally enhanced even at higher WC loadings. The optimal balance appears around 10–20% WC, where strength gains are significant without compromising elongation. The data confirms that WC reinforcement effectively strengthens aramid composites while retaining sufficient flexibility (Figure 9).

CONCLUSION

The experimental analysis on aramid fiber-reinforced epoxy composites with varying tungsten carbide filler content (5%, 10%, 15%, and 20%) has demonstrated a notable impact regarding the mechanical characteristics of composite materials. Among all compositions, the specimen reinforced with 20% tungsten carbide exhibited the highest average tensile strength of 359.68 N/mm² and a corresponding peak load of 22.48 kN, indicating significant improvement over the baseline and lower

filler ratios. A progressive increase in load at peak and tensile strength was observed with the increase in tungsten carbide content up to 20%, along with relatively consistent elongation at break, suggesting the effective load transfer and enhanced stiffness imparted by the ceramic reinforcement. The composite with 15% WC, despite showing moderate tensile strength (322.88 N/mm²), recorded the highest elongation at break (11.424 mm), indicating a balanced ductility-stiffness behavior. Furthermore, the results confirm that filler dispersion and fiber-matrix bonding are critical to achieving optimal mechanical performance. The data supports that 20% WC is the most effective concentration for maximizing strength without significantly compromising ductility, making it suitable for applications requiring high tensile and impact resistance. These findings validate the potential of tungsten carbide as a reinforcing filler in aramid-epoxy composites, especially for structural and protective components where both strength and durability are essential.

REFERENCES

1. S. Sajan and D. Philip Selvaraj, "A review on polymer matrix composite materials and their applications," Materials Today: Proceedings, vol. 47, pt. 15, pp. 5493–5498, 2021, doi: 10.1016/j.matpr.2021.08.034.
2. A. K. Bledzki and J. Gassan, “Composites reinforced with cellulose based fibres,” *Prog. Polym. Sci.*, vol. 24, no. 2, pp. 221–274, 1999. doi: 10.1016/S0079-6700(98)00018-7.
3. C. Soutis, "Fibre reinforced composites in aircraft construction," Progress in Aerospace Sciences, vol. 41, no. 2, pp. 143–151, 2005, doi: 10.1016/j.paerosci.2005.02.004.
4. A. Rashidi, J. P.-H. Belnoue, A. J. Thompson, S. R. Hallett, and A. S. Milani, "Consolidation-driven wrinkling in carbon/epoxy woven fabric prepregs: An experimental and numerical study," Composites Part A: Applied Science and Manufacturing, vol. 143, 106298, 2021, doi: 10.1016/j.compositesa.2021.106298.
5. G. Soni, S. Gupta, R. Singh, M. Mitra, W. Yan, and B. G. Falzon, "Study of localized damage in composite laminates using micro–macro approach," Composite Structures, vol. 113, pp. 1–11, 2014, doi: 10.1016/j.compstruct.2014.02.016.
6. T. Sinmazçelik, E. Avcu, M. Ö. Bora, and O. Çoban, "A review: Fibre metal laminates, background, bonding types and applied test methods," Materials & Design, vol. 32, no. 7, pp. 3671–3685, 2011, doi: 10.1016/j.matdes.2011.03.011.
7. F. Mustata and N. Tudorachi, "Curing kinetics and thermal characterization of epoxy resin cured with amidodicarboxylic acids," Applied Thermal Engineering, vol. 125, pp. 285–296, 2017, doi: 10.1016/j.applthermaleng.2017.07.037.
8. P. Parvizi, M. Jalilian, and K. D. Dearn, "Epoxy composites reinforced with nanomaterials and fibres: Manufacturing, properties, and applications," Polymer Testing, vol. 146, 108761, 2025, doi: 10.1016/j.polymertesting.2025.108761.
9. N. Shukla and G. L. Devnani, "A review on mechanical properties of hybrid natural fiber polymer composites," Materials Today: Proceedings, vol. 45, pt. 6, pp. 4702–4705, 2021, doi: 10.1016/j.matpr.2021.01.122.
10. E. George, J. Joy, P. V. Poornima, H. Vahabi, S. C. George, and S. Anas, "Effect of filler loading on the frictional, thermal and mechanical properties of ABS/boron nitride (h-BN) nanocomposites," Nano-Structures & Nano-Objects, vol. 40, 101372, 2024, doi: 10.1016/j.nanoso.2024.101372.
11. C. Elanchezhian, B. V. Ramnath, G. Ramakrishnan, M. Rajendrakumar, V. Naveenkumar, and M. K. Saravanakumar, "Review on mechanical properties of natural fiber composites," Materials Today: Proceedings, vol. 5, no. 1, pt. 1, pp. 1785–1790, 2018, doi: 10.1016/j.matpr.2017.11.276.
12. M. Ramesh, K. Palanikumar, and K. H. Reddy, "Mechanical property evaluation of sisal–jute–glass fiber reinforced polyester composites," Composites Part B: Engineering, vol. 48, pp. 1–9, 2013, doi: 10.1016/j.compositesb.2012.12.004.
13. B. Wetzel, F. Haupert, and M. Q. Zhang, "Epoxy nanocomposites with high mechanical and tribological performance," Composites Science and Technology, vol. 63, no. 14, pp. 2055–2067, 2003, doi: 10.1016/S0266-3538(03)00115-5.

14. S. K. Shubham, R. Purohit, P. S. Yadav, and R. S. Rana, "Study of nano-fillers embedded in polymer matrix composites to enhance its properties – A review," Materials Today: Proceedings, vol. 26, pt. 2, pp. 3024–3029, 2020, doi: 10.1016/j.matpr.2020.02.629.
15. M. K. Reddy, V. S. Babu, K. V. S. Srinadh, and M. Bhargav, "Mechanical properties of tungsten carbide nanoparticles filled epoxy polymer nano composites," Materials Today: Proceedings, vol. 26, pt. 2, pp. 2711–2713, 2020, doi: 10.1016/j.matpr.2020.02.569.
16. P. Manvi et al., "Stress Based Topology Optimization of Axial Tubes Under Impact to Improve Energy Absorption," *J. Polym. Compos.*, vol. 12, Special Issue 4, pp. S210–S220, 2024. doi: 10.59360/jopc.2024145848.
17. P. Manvi et al., "Designing of a Long-Range Autonomous Multirotor on a Custom-Built Carbon Fiber Frame," in *Recent Advances in Mechanical Engineering, Lecture Notes in Mechanical Engineering*, Springer Nature Singapore Pte Ltd., 2023. doi: 10.1007/978-981-19-1388-4_9.
18. B. P. Mishra, D. Mishra, P. Panda, and A. Maharana, "An experimental investigation of the effects of reinforcement of graphene fillers on mechanical properties of bi-directional glass/epoxy composite," Materials Today: Proceedings, vol. 33, pt. 8, pp. 5429–5441, 2020, doi: 10.1016/j.matpr.2020.03.154.
19. P. A. Anandh, P. Sivabalan, V. Mohanavel, and T. Raja, "Investigation of basalt/kevlar fiber-reinforced porcelain filler infused epoxy composite: A viable alternative for marine applications," Results in Engineering, vol. 25, 103928, 2025, doi: 10.1016/j.rineng.2025.103928.
20. K. P. Srinivasa Perumal, L. Selvarajan, K. P. Manikandan, and C. Velmurugan, "Mechanical, tribological, and surface morphological studies on the effects of hybrid ilmenite and silicon dioxide fillers on glass fibre reinforced epoxy composites," *Journal of the Mechanical Behavior of Biomedical Materials,* vol. 146, 106095, 2023, doi: 10.1016/j.jmbbm.2023.106095.
21. S. Kar, S. Pattnaik, and M. K. Sutar, "Assessment of mechanical and thermal properties of hybrid co-woven biofiber polymer composites," Industrial Crops and Products, vol. 222, pt. 3, 119756, 2024, doi: 10.1016/j.indcrop.2024.119756.
22. K. Gopala Krishna, C. Divakar, K. Venkatesh, C. B. Mohan, and K. S. M. Lohith, "Tribological studies of polymer based ceramic–metal composites processed at ambient temperature," Wear, vol. 266, no. 7–8, pp. 878–883, 2009, doi: 10.1016/j.wear.2008.08.013.
23. N. Kumar, P. K. Patnaik, S. K. Mishra, G. K. Mohanta, and M. R. Panda, "Mechanical and tribological properties of Al7075 based metal matrix composite reinforced with boron carbide and blast furnace slag," Materials Today: Proceedings, 2023, doi: 10.1016/j.matpr.2023.12.037.
24. Y. Wang, A. Li, L. Shu, and J. Qin, "The effect of WC addition on the microstructure and properties of laser cladded Ni-WC coatings," Materials Today Communications, vol. 46, 112515, 2025, doi: 10.1016/j.mtcomm.2025.112515.
25. M. Ostolaza, J. I. Arrizubieta, A. Lamikiz, and E. Ukar, "Study of the flexural behaviour and bonding strength of WC-Co metal matrix composite coatings produced by Laser Directed Energy Deposition," Surface and Coatings Technology, vol. 463, 129538, 2023, doi: 10.1016/j.surfcoat.2023.129538.
26. H. A. Dahish and A. D. Almutairi, "Effect of elevated temperatures on the compressive strength of nano-silica and nano-clay modified concretes using response surface methodology," Case Studies in Construction Materials, vol. 18, e02032, 2023, doi: 10.1016/j.cscm.2023.e02032.
27. Y. Rostamiyan, A. Fereidoon, A. H. Mashhadzadeh, M. R. Ashtiyani, and A. Salmankhani, "Using response surface methodology for modeling and optimizing tensile and impact strength properties of fiber orientated quaternary hybrid nano composite," Composites Part B: Engineering, vol. 69, pp. 304–316, 2015, doi: 10.1016/j.compositesb.2014.09.031.

